CONF-8908146--16

UCRL-98850

Preprint

DO NOT MICROFILM
COVER

Received by OSTI
JUL 1 0 1989

Tapering FEL Amplifiers in Wiggler Period and Field

H. D. Shay, G. A. Deis,
E. T. Scharlemann, and
T. E. Smith, Jr.
Lawrence Livermore
National Laboratory

Prepared for presentation at the
10th International Free-Electron
Laser Conference
Jerusalem, Israel
August 28–September 2, 1988

March 13, 1989

Beam Research Program

Lawrence Livermore National Laboratory

This is a preprint of a paper intended for publication in a journal or proceedings. Since changes may be made before publication, this preprint is made available with the understanding that it will not be cited or reproduced without the permission of the author.

DISTRIBUTION OF THIS DOCUMENT IS UNLIMITED

MASTER

DISCLAIMER

This report was prepared as an account of work sponsored by an agency of the United States Government. Neither the United States Government nor any agency thereof, nor any of their employees, makes any warranty, express or implied, or assumes any legal liability or responsibility for the accuracy, completeness, or usefulness of any information, apparatus, product, or process disclosed, or represents that its use would not infringe privately owned rights. Reference herein to any specific commercial product, process, or service by trade name, trademark, manufacturer, or otherwise does not necessarily constitute or imply its endorsement, recommendation, or favoring by the United States Government or any agency thereof. The views and opinions of authors expressed herein do not necessarily state or reflect those of the United States Government or any agency thereof.

DISCLAIMER

Portions of this document may be illegible in electronic image products. Images are produced from the best available original document.

Tapering FEL Amplifiers in Wiggler Period and Field*

H. D. Shay, G. A. Deis, E. T. Scharlemann, and T. E. Smith, Jr.
Lawrence Livermore National Laboratory
Livermore, California 94550

Presentation at the Tenth International Free Electron Laser Conference
Jerusalem, Israel
August 28-September 2, 1988

UCRL--98850

DE89 014050

Abstract

Tapering a free-electron laser (FEL) amplifier to improve extraction after gain saturation can be accomplished by varying both the wiggler period and the wiggler field. This paper considers specific FEL designs and demonstrates the improvement in extraction efficiency that can be achieved by utilizing both variations. Fabrication considerations make a continuously varying wiggler period impractical for long wigglers, and so this technique entails discontinuous steps in the wiggler period. Such steps in wiggler period must be introduced in a manner such that they do not induce steering in the electron beam for reasonable ranges of transverse velocities and energies nor induce a large spread in phase shifts. We discuss such techniques.

---

* Performed jointly under the auspices of the U.S. DOE by LLNL under W-7405-ENG-48 and under the auspices of the U.S. DOD under SDIO/SDC-ATC MIPR No. W31-RPD-9-D5007.

DISTRIBUTION OF THIS DOCUMENT IS UNLIMITED

MASTER

I. Introduction

In this paper, we discuss one dilemma that we confront when tuning a free-electron laser (FEL) amplifier: the fact that the optimal-choice wiggler period for trapped particle deceleration may result in poor trapping efficiency. We also examine one possible solution: simultaneous tapering in both the wiggler period and field. This tapering scheme was suggested previously in Refs. [1, 2, and 3]. Here, we consider the detailed implementation required for a high-efficiency FEL. We show that simultaneous wiggler tapering together with corrective beam steering offset a variety of FEL degradation mechanisms.

Several mechanisms can degrade FEL performance (e.g., low-electron beam brightness, random wiggler field errors, jitter or slew in electron beam energy, jitter in electron beam position at the entrance to the wiggler, and instantaneous energy spread). In this paper, we focus on the first two mechanisms listed. (Reference [4] contains a more detailed discussion of all these mechanisms and presents alternative methods for mitigating their effects.)

To illustrate the effects of degradation and the compensation for these effects afforded by simultaneous tapering, we selected a numerical example that has marginal performance caused by a combination of three degradation mechanisms: low electron-beam brightness, low beam energy, and wiggler errors. The nominal operating conditions for all the examples cited in this paper are shown in Fig. 1. We used the computer code FR3D (the 3D version of FRED [5]) for these numerical simulations. This code has a fully three-dimensional, Monte Carlo treatment of electron betatron

motion and follows the first five (m = 0, ±1, and ±2) azimuthal modes of the laser light.

II. Discussion

To illustrate the fundamental reason why simultaneous tapering enhances extraction efficiency, we resort to using a simple model in which the extraction efficiency is the product of the electron capture efficiency into the ponderomotive well and the subsequent efficiency of deceleration of those captured electrons:

$$\eta_x = \eta_c \, \eta_d.$$

A simplified view of trapping suggests that the capture efficiency varies as the overlap of the electron initial phase-space distribution and the ponderomotive bucket. Using the expression for the bucket area from KMR [1],

$$A_{bucket} \approx 8\gamma_r \sqrt{\frac{a_s a_w}{1+a_w^2}} \quad ,$$

and taking the spread in γ to result exclusively from the betatron $\beta_\perp$,

$$\frac{\delta\gamma_{||}}{\gamma_{||}} \approx \frac{\varepsilon_N \, k_w \, a_w}{1 + a_w^2} \quad ,$$

we find that, for a spread in $\gamma_{||}$ large compared with the height of the ponderomotive bucket and for a_w slightly greater than one,

$$\eta_c \equiv \frac{A_{bucket}}{2\pi\ \delta\gamma_{||}} \sim \frac{2\gamma_0^2\,\lambda_s\lambda_w^{1/4}}{\left(2\gamma_0^2\,\lambda_s - \lambda_w\right)^{1/4}}\sqrt{a_s}\,\sqrt{\frac{J}{I}}\ .$$

Here, J is the electron beam brightness, I is the beam current, λ_s is the laser wavelength, λ_w is the wiggler period, γ_0 is initial electron beam gamma, A_{bucket} is the area of the ponderomotive bucket in phase space, and $\delta\gamma_{||}$ is the width of the electron beam distribution in

$$\gamma_{||} = \gamma/\mu = \frac{\gamma}{\sqrt{1+a_w^2+a_s^2}}\ .$$

In the extreme case of large magnetic scalar potential,

$$a_w = \sqrt{\frac{2\gamma_0^2\lambda_s}{\lambda_w} - 1}\ ,$$

the capture fraction becomes

$$\eta_c \sim \lambda_w\ \sqrt{\frac{J}{I}}\ .$$

Likewise, we have derived a simple 1D model from the KMR period averaged equations [1]. For an amplifier tapered to maintain no change in the phase angle ψ_0, we can obtain an equation for the laser's electric-field strength as a function of distance along the FEL, z. For large z, well into

the tapered regime, the growth of the deceleration efficiency η_d can then be found to be

$$\frac{d\eta_d}{dz} \propto \sqrt{\frac{2\lambda_s\gamma_0}{\lambda_w}}\left(\frac{2\lambda_s\gamma_0}{\lambda_w} - \frac{1}{\gamma_0}\right)\sqrt{J_c} \approx \gamma_0^{3/2}\left(\frac{\lambda_s}{\lambda_w}\right)^{3/2}\sqrt{J_c} \ ,$$

where J_c is the captured current density. For an electron beam well matched to the acceptance of the wiggler,

$$J_c \cong \frac{\eta_c I}{\pi\, r_b^2} \propto \frac{2\gamma_0^3\lambda_s^{3/2} J\sqrt{a_s}}{\lambda_w^{5/4}\left(2\gamma_0^2\lambda_s - \lambda_w\right)^{1/4}} \ .$$

We then have

$$\frac{d\eta_d}{dz} \propto \gamma_0^3\sqrt{J}\,\frac{\lambda_s^3}{\lambda_w^{13/8}}\,\frac{a_s^{1/4}}{\left(2\gamma_0^2\lambda_s - \lambda_w\right)^{1/8}} \ ,$$

and, for

$$\frac{2\gamma_0{}^2\lambda_s}{\lambda_w} >> 1 \text{ or } a_w >> 0,$$

$$\frac{d\eta_d}{dz} \propto \gamma_0^{11/4}\sqrt{J}\sqrt{a_s}\,\frac{\lambda_s^{23/8}}{\lambda_w^{13/8}} \ .$$

Likewise, we know from the resonance condition that the maximum deceleration efficiency, attained when the wiggler field has been tapered nearly to zero, is

$$\eta_d = \frac{1}{\gamma_o}\left(\gamma_o - \sqrt{\frac{\lambda_w}{2\,\lambda_s}}\right).$$

Whereas the capture efficiency would prompt the use of a long wiggler period, the deceleration efficiency would favor instead a short wiggler period.

This exceedingly simplistic model qualitatively reflects the results of our computer calculations. FRED simulations, conducted with a range of wiggler periods (the constant λ_w curve in Fig. 2), illustrate that the extraction efficiency falls to zero for both the long and short wiggler periods as either the deceleration or capture efficiency, respectively, vanishes. For this laser wavelength and electron energy, the critical wiggler period value (the value for which the magnetic field vanishes, $\lambda_w = 2\gamma^2\,\lambda_s$) is 15 cm, as indicated. In these calculations, as the energy of a designated tuning particle diminishes, the magnetic field is tuned along the length of the wiggler to preserve a constant ψ for this particle, as shown by the solid line in Fig. 3a.

An alternative tapering scheme is to vary both the wiggler field and period. We have placed the wholly arbitrary constraint of the λ_w varying linearly along the length of the wiggler with the magnetic field, assuming whatever value that is needed to preserve constant ψ for the tuning particle. In the simulations labeled in Fig. 2 as "tapered λ_w," we constrained the wiggler period to the value of the abscissa at the

beginning of the wiggler and to 2 cm at the end of the wiggler. Although the trapped particle fraction is typically lower than the comparable constant period FEL (Fig. 3c), this loss is greatly offset by the increase in extraction efficiency (Fig. 3b). Effectively, the smaller period at the end of the wiggler permits the wiggler vector potential to remain large for a far greater length than is possible for a constant period FEL as shown in Fig. 3a.

In these FEL simulations, we assumed that λ_w is continuously varying, a condition that is scarcely practicable. The condition that a sequence of poles would have a non-steering pattern of excitation would be far harder to realize than with the constant λ_w that employ binomial patterns of excitation [6]. Each coil would have to be custom wound with the concomitant increase in cost and in the likelihood of fabrication errors. Finally, once wiggler errors were detected, the procedures for eliminating them would be much more complicated.

One alternative to a continuously tapered wiggler period is to have the wiggler period changed in steps--that is, constant for some distance and then jumped to a lower value. FRED simulations indicate that a large number of steps, fifteen or more, are required to approximate a continuously tapered λ_w. A few of the steps have large jumps between successive values of λ_w, and these jumps produce detrapping of the captured electrons. The problem of tapering λ_w can, in principle, be reduced to the question of finding ways of producing jumps which, for any reasonable value of γ or $\beta_\perp$, will advance the phase angle ψ by a small multiple of 2π and will be non-steering. Figure 4 illustrates the pole excitations both for the case having a field free "drift space" between the two wiggler sections and for the case with the transitional region having

poles spaced with graded intervals. In the case with a drift space, the entrance and exit patterns on the wiggler sections should have the usual binomial excitation pattern to satisfy the non-steering condition and should have the length of the drift space tuned to meet the $n(2\pi)$ conditions on the phase angle jump.

A straightforward derivation based on the KMR equations [1] indicates the change in phase expected in traversing such a drift space. In the KMR equation for $\frac{d\psi}{dz}$, we set the terms with a_w approximately to zero in the drift space and also neglect the small a_s^2 and $\frac{d\phi}{dz}$ terms:

$$\frac{d\psi}{dz} = k_w - \frac{k_s}{2\gamma^2}\left[1 + a_w^2 + \gamma^2\beta_{\perp,\beta}^2 - 2a_w f_B a_s \cos\psi + a_s^2\right] + \frac{d\phi}{dz} \cong k_w - \frac{k_s}{2\gamma^2}\left[1 + \gamma^2\beta_{\perp,\beta}^2\right] .$$

If the last pole of the λ_1 pattern before the drift space has its center at z_1 and the first pole of the new λ_2 pattern has its center at z_2, then the phase of an electron at arriving at z_2 may be expressed in terms of its phase at z_1:

$$\psi(z_2) \cong \psi(z_1) + \Delta z \left(k_{w_1} - \frac{k_s}{2\gamma^2}\left[1 + \gamma^2\beta_{\perp,\beta}^2\right]\right) + \delta\psi \ ,$$

where Δz is the width of the drift space, z_2-z_1. The term $\delta\psi$ arises because of the need to shift the definition of ψ from the λ_1 pattern to the λ_2 pattern and is just

$$\delta\psi \equiv -k_{w_1}(\Delta z - n\lambda_1) \ ,$$

where n is the largest integer such that $\Delta z \geq n\lambda_1$. Since differences in ψ of multiples are not relevant, we find

$$\Delta\psi \equiv \psi(z_2) - \psi(z_1) \approx \text{constant} - \Delta z \frac{k_s}{2\gamma^2}\left(1 + \gamma^2 \beta_{\perp,\beta}^2\right).$$

This result is independent of which end of the drift space is used as the reference point for ψ.

For the case of the transitional poles, there is an infinite set of pole spacings and associated pole excitations that will produce a non-steering pattern. In the example displayed in Fig. 4, the pole spacing varies linearly between $\lambda_{w1}/2$ and $\lambda_{w2}/2$. With this choice of pole spacing, there is a unique pattern of relative pole excitation that will not steer the electron beam; the jump in the phase angle ψ is tuned by scaling the entire excitation pattern. In a derivation similar to the one for the drift space, we can show that

$$\Delta\psi \approx \text{constant} - \Delta z \frac{k_s}{2\gamma^2}\left(1 + \gamma^2 \beta_{\perp,\beta}^2\right) - \frac{k_s B_{MAX}^2}{2\gamma^2}\int_{z_1}^{z_2} \frac{b_y^2}{k_w^2}\, dz ,$$

where B_{max} is magnetic scaling factor for the transitional pattern.

In order to elucidate the statements made above, we examined the field patterns of each case and the trajectories and phase space evolution of traversing electrons. To simplify this exercise, without weakening the conclusions, we considered a 2D system translationally invariant in x. We used the 2D computer code POISSON to solve for the B_y and B_z fields in the yz plane ($B_x = 0$) for each of these two cases. The motion of the electrons

was studied with the 3D Monte Carlo (MC) trajectory code FRET. Unlike FRED, FRET solves for the detailed wiggle motion (5th order Runge-Kutta solver for accuracy), but it does not follow the laser beam and so it has no ponderomotive forces acting on the electrons. In these cases, because the fields were taken from 2D POISSON, FRET was used with the wiggle motion in the xz plane and with the betatron motion only in yz plane. In these simulations, we have assumed that the average electron in the beam is initially in resonance in the first wiggler section and that its emittance is properly matched to the wiggler acceptance.

Figure 5 depicts the B_y along the axis of the wiggler both for the drift space of Fig. 4 and for the transitional region. In wiggler sections on either side, the magnetic field is tuned to be in resonance for 30 MeV. Also to either side, the excitation patterns of the poles have a non-steering 4:3:1 pattern. It is clear from Fig. 5b that the field of the transitional section adds to the fringing fields of the wiggler sections to either side. The magnitude of the field in this transitional section is varied to tune the $\Delta\psi$ jump, as indicated by the solid and dashed lines for the field in the transitional region. The FRET calculations of electron trajectories in these two fields are shown in Fig. 6a and b. The consequence of not using a binomial pattern in entrance and exit sections is illustrated in Fig. 6c, where the electron trajectory is severely steered in traversing the gap.

We used FRET to verify the statements made above concerning the tuning of the $\Delta\psi$ across each of these transitional gaps. Figure 7a and b depicts the jump in phase angle averaged over a collection of MC particles for each of these two for a sequence of tuning conditions. In Fig. 7a, the width of the drift space Δz is varied, and the result expected from the

simple expression above is obtained. Likewise, for the "transitional" section, the maximum magnetic field is used in tuning, again with the expected result.

A spread in the longitudinal energy, arising either from a spread in the energy or from betatron amplitude, results in a spread in the jump imparted in phase in traversing either kind of interface between wiggler sections with different periods. Figure 8 shows the MC results from FRET for the "transitional" section example. Here, the intrinsic energy spread $d\gamma/\gamma$ is relatively small and most of the dispersion in phase angle results from the spread in betatron amplitude. Since r_b is proportional to the invariant betatron transverse velocity for each electron, and since the expression for $\Delta\psi$ includes a $\beta_\perp{}^2$ term, the dispersion in $\Delta\psi$ is quadratic in r_b.

This unavoidable dispersion in $\Delta\psi$ results in particles leaking from the ponderomotive bucket each time the wiggler period is changed. As shown in Table 1, the extraction efficiency realized with variable λ_w with dispersive sections between λ_w sections, 11.3%, is poorer than with idealized interfaces, 14.6%. In this example, selected to emphasize the improvement possible with simultaneous tapering, the improvement estimated from these more realistic models is distinctly poorer than that estimated from the simple model of continuous λ_w variation.

III. Conclusions

In this paper, we have examined the technique of simultaneously tapering the wiggler in magnetic field and period as a possible solution to offset such performance-degrading mechanisms as random wiggler field

errors. We found that successful application of this technique necessitates the use of many distinct wiggler sections of different periods separated by tunable transitional regions. Even with perfect tuning of the transitional regions, some inescapable detrapping of the captured electrons occurs at the interface between wiggler sections.

References

[1] N. M. Kroll, P.L. Morton, and M. N. Rosenbluth, "Free-Electron Lasers with Variable Parameters Wigglers," IEEE J. Quant. Elec., QE-17 (1981), 1436.

[2] D. Prosnitz, A. Szoke, and V. K. Neil, "High-Gain, Free-Electron Laser Amplifier: Design considerations and Simulation," Phys. Rev. A 24 (1981), 1436.

[3] R. A. Cover and A. Bhomik, "Enhanced Performance from High-extraction-efficiency Free Electron Lasers," Nuclear Instruments and Methods in Physics Research A272 (1988), 117.

[4] H.D. Shay and E. T. Scharlemann, "Reducing Sensitivity to Errors in Free Electron Laser Amplifiers," Nuclear Instruments and Methods in Physics Research A272 (1988), 601.

[5] E.T. Scharlemann and W.M. Fawley, SPIE Symp. on Optics and Optoelectronics Systems (1986), Lawrence Livermore National Laboratory, Livermore Calif. Report UCRL-94258.

[6] K. Halbach, "Desirable Excitation Patterns for Tapered Wigglers," Nuclear Instruments and Methods in Physics Research A250 (1986), 95.

Table 1. Extraction efficiency for several tapering schemes.

Case	Extraction efficiency
Constant λ_w = 12 cm	5.2%
Smoothly tapered λ_w (12 to 2 cm)	≤14.6%
λ_w tapered with steps	≤12.2%
λ_w tapered with steps having dispersive coupling between λ_w sections	≤11.3%

List of Figures

1. Extraction efficiency is plotted versus electron brightness for low electron beam energy. The parameters of the FR3D simulations appear to the right of the graph.

2. Extraction efficiency is plotted versus initial wiggler period. Two sets of simulations are shown: one in which the wiggler period remains constant at the initial value and only the magnetic field is tapered, and one in which the wiggler period is linearly tapered from the initial value to 2 cm at the end of the wiggler while the field is varied simultaneously to maintain the resonance condition. All other FEL parameters are the "nominal conditions" shown in Fig. 1.

3. These graphs illustrate the contrast in FELs with tapering in magnetic field only or in both period and field. Plot (a) depicts the normalized vector potential as a function of distance along the length of the wiggler; (b) , the variation of the capture fraction; (c) , the extraction efficiency.

4. This figure shows the relative field excitation to the poles at the interface between a wiggler section with period 10 cm and one with 9 cm. Each section has second-order steering free-excitations: one power supply excites four poles with a ratio of turns of 1:3:3:1. The poles between the two sections are spaced in a manner which varies smoothly from 5 to 4 cm. One possible set of non-steering excitations for these poles is shown: 1:3.035:3.025:1. When this interface is treated as a drift space, the power supply for these transitional poles would be turned off.

5. These plots show the y component of the magnetic field for (a) a "drift" space and (b) a "transitional" region. Note that the magnetic field in the transitional region is the sum of the fields from the

sections on either side and from the poles in the transitional space. This later field is tuned for the condition on $\Delta\psi$.

6. These are the trajectories for an electron with initial $x' = y = y' = 0$ crossing the interface between two wiggler sections. The trajectory (a) corresponds to the drift or dispersion section of Fig. 5a; trajectory (b), to the transitional section of Fig. 5b. The consequence of not having non-steering patterns on the exit and entrance of the wiggler sections is illustrated in (c).

7. These plots depict $\Delta\psi$, averaged over a random distribution of electrons, as a function of the length of the drift space for a dispersion section, (a), or as a function of the peak magnetic field in transitional section, (b).

8. The graph shows $\Delta\psi$ for a collection of electrons as a function of their betatron amplitude. A random variation in energy, $\delta\gamma$, also contributes to a variation in longitudinal velocity and, hence, to a spread in $\Delta\psi$.

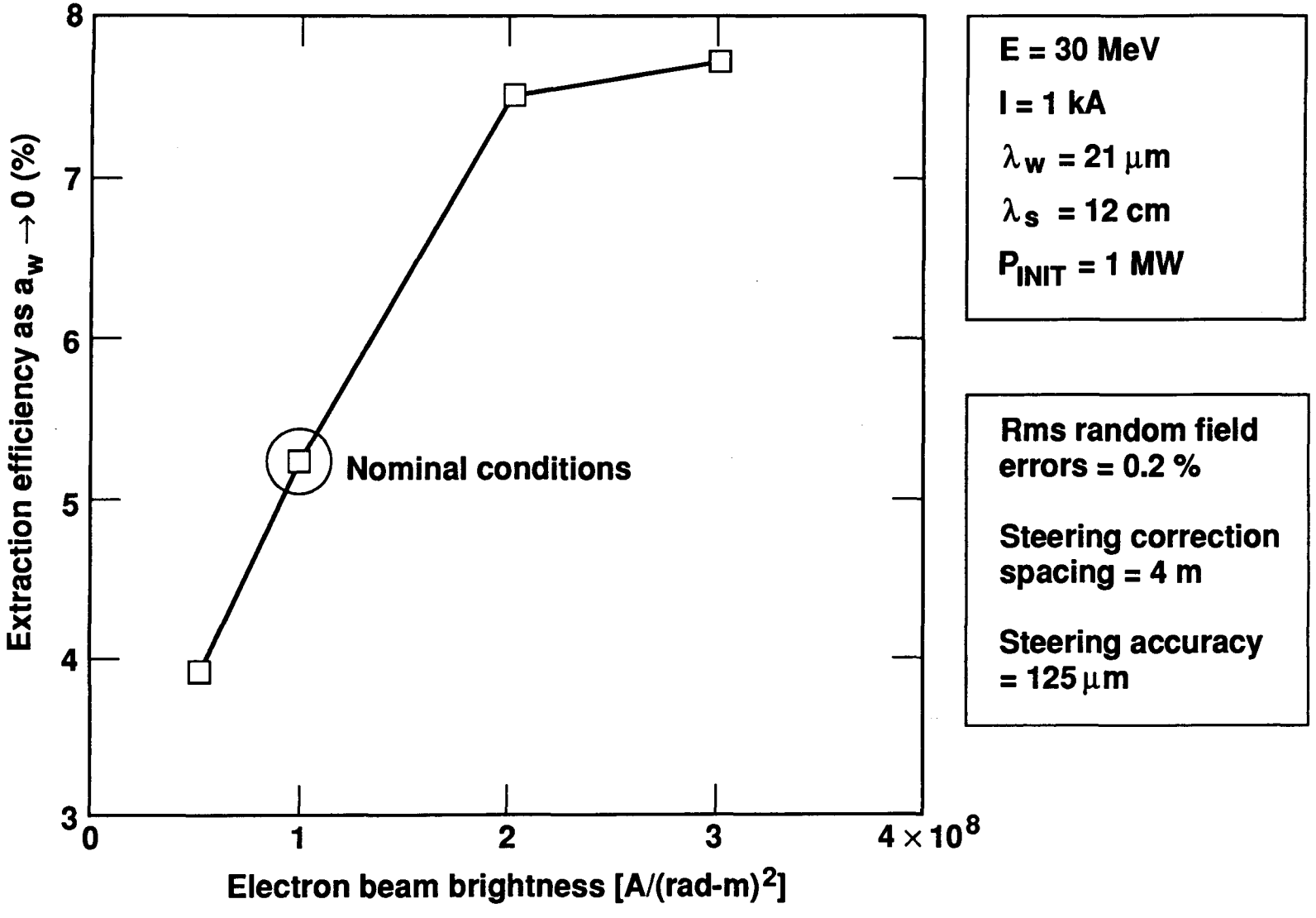
Extraction efficiency as $a_w \rightarrow 0$ (%)
8
7
6
5
4
3
0
1
2
3
4×10^8
Electron beam brightness [A/(rad-m)^2]
Nominal conditions
E = 30 MeV
I = 1 kA
λ_w = 21 μm
λ_s = 12 cm
P_{INIT} = 1 MW
Rms random field errors = 0.2 %
Steering correction spacing = 4 m
Steering accuracy = 125 μm

Fig. 1

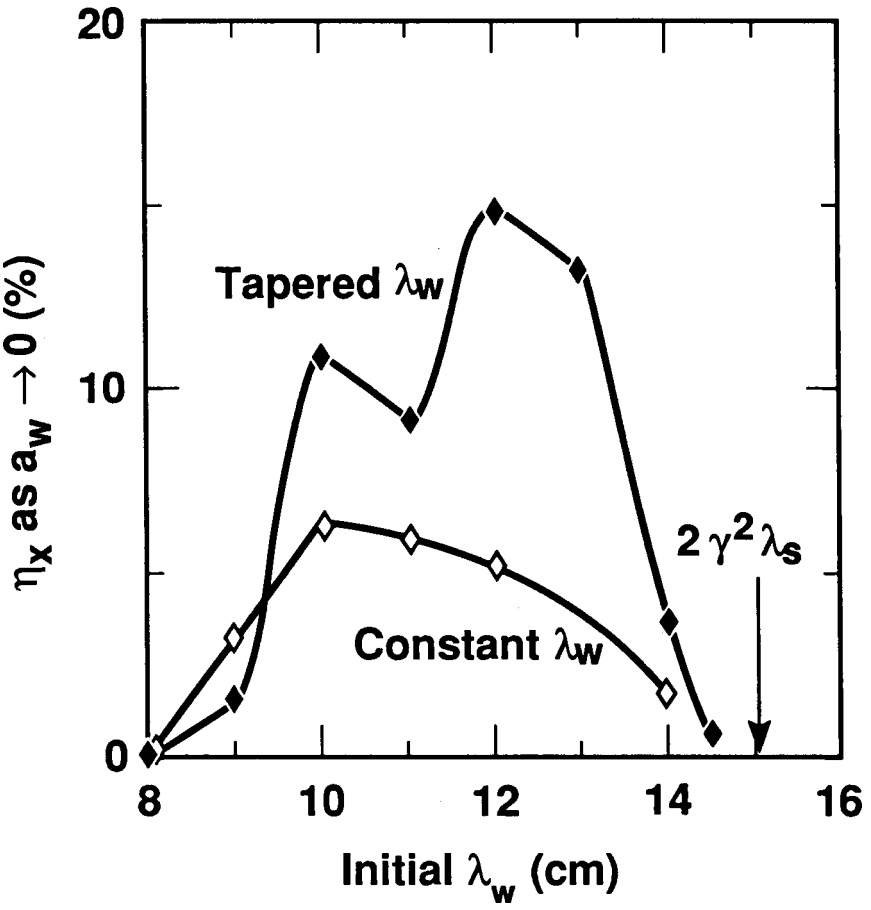

80-X-0289-0056-1

Fig. 2

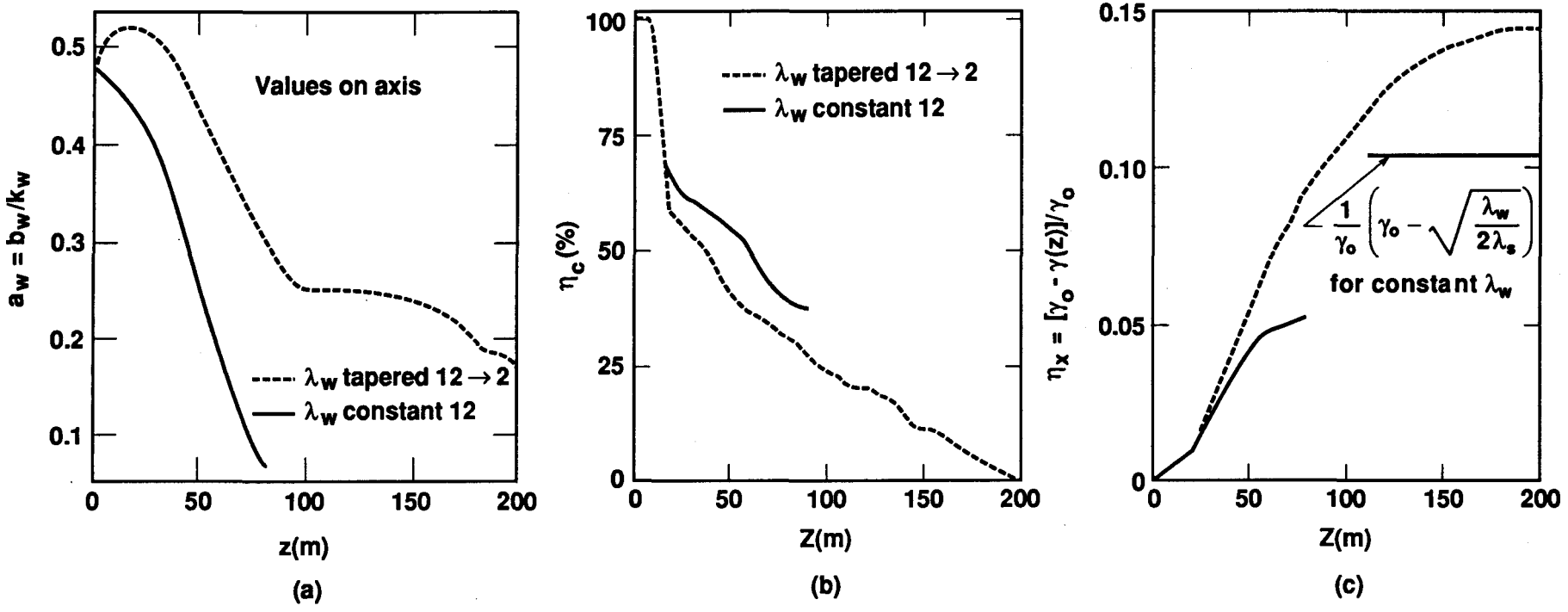
0.5
0.4
0.3
0.2
0.1
$a_w = b_w/k_w$
Values on axis
λ_w tapered 12 → 2
λ_w constant 12
0
50
100
150
200
z(m)
(a)
100
75
50
25
0
η_c (%)
λ_w tapered 12 → 2
λ_w constant 12
0
50
100
150
200
Z(m)
(b)
0.15
0.10
0.05
0
$\eta_x = [\gamma_o - \gamma(z)]/\gamma_o$
$\frac{1}{\gamma_o}\left(\gamma_o - \sqrt{\frac{\lambda_w}{2\lambda_s}}\right)$
for constant λ_w
0
50
100
150
200
Z(m)
(c)

Fig. 3

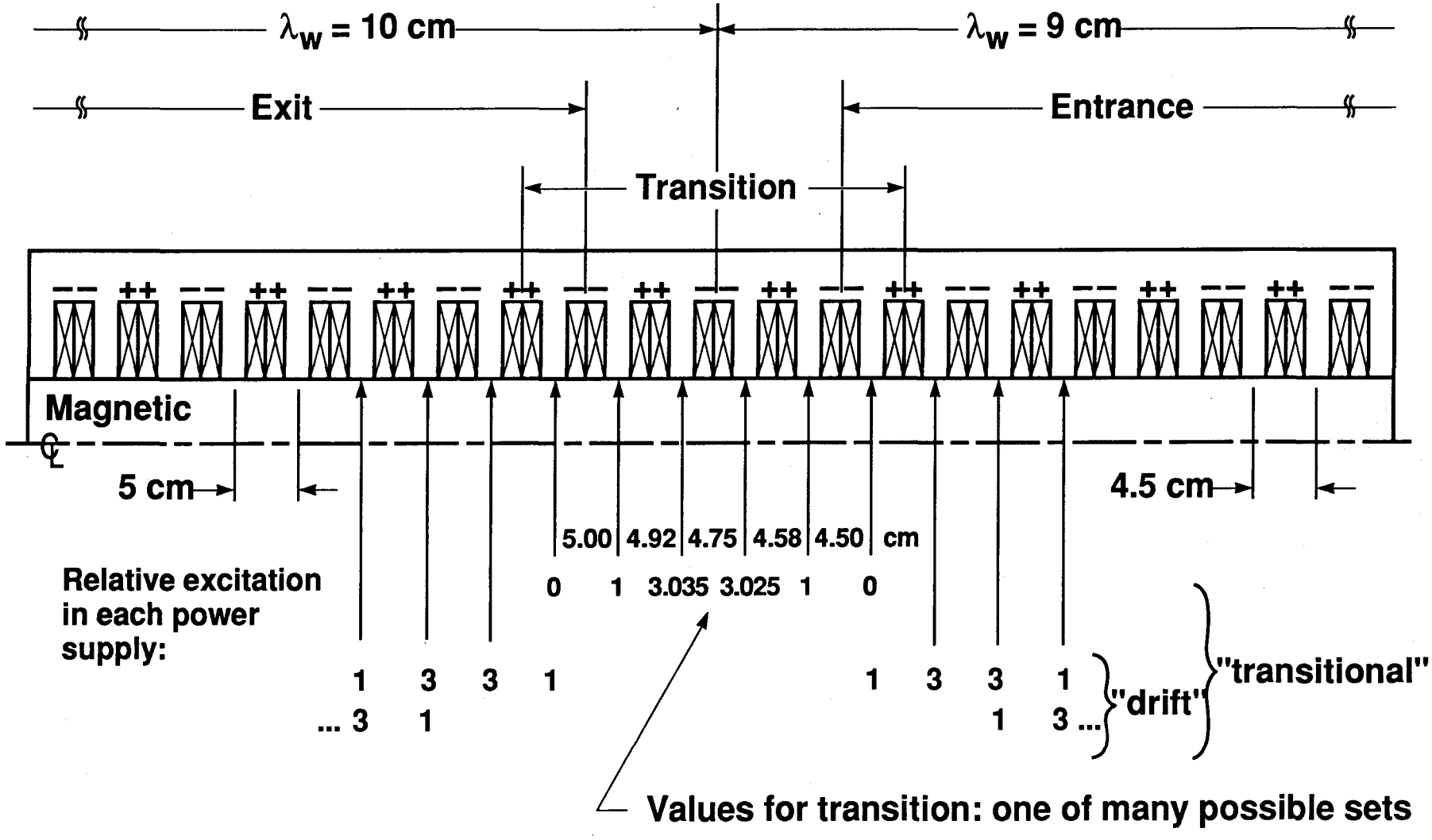
λw = 10 cm
λw = 9 cm
Exit
Entrance
Transition
Magnetic
℄
5 cm
4.5 cm
5.00 4.92 4.75 4.58 4.50 cm
Relative excitation in each power supply:
0 1 3.035 3.025 1 0
1 3 3 1 1 3 3 1
... 3 1 1 3 ...
"drift"
"transitional"
Values for transition: one of many possible sets

Fig. 4

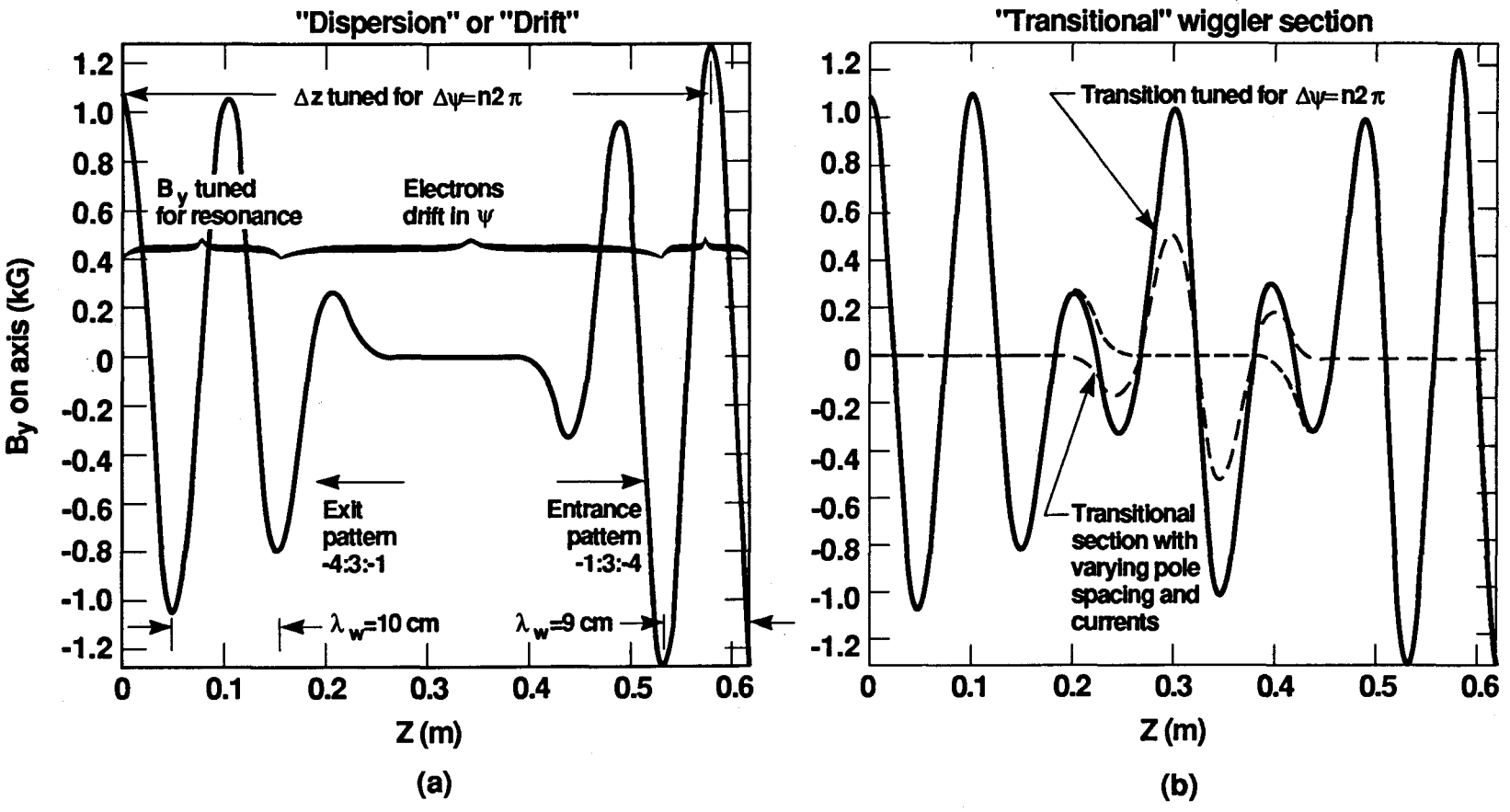
"Dispersion" or "Drift"
Δz tuned for Δψ=n2π
B y tuned for resonance
Electrons drift in ψ
Exit pattern -4:3:-1
Entrance pattern -1:3:-4
λ w=10 cm
λ w=9 cm
By on axis (kG)
Z (m)
(a)
"Transitional" wiggler section
Transition tuned for Δψ=n2π
Transitional section with varying pole spacing and currents
Z (m)
(b)

Fig. 5

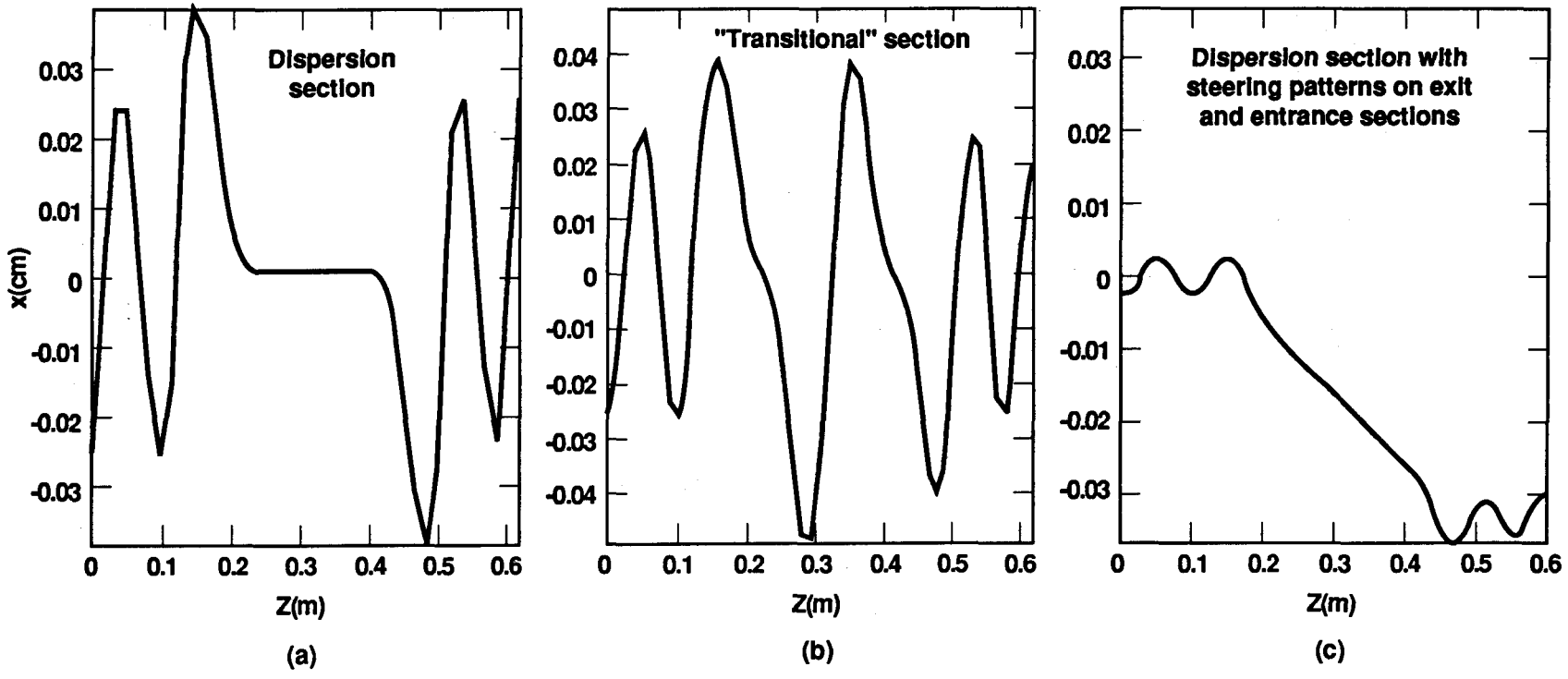
Dispersion section
x(cm)
0.03
0.02
0.01
0
-0.01
-0.02
-0.03
0 0.1 0.2 0.3 0.4 0.5 0.6
Z(m)
(a)
"Transitional" section
0.04
0.03
0.02
0.01
0
-0.01
-0.02
-0.03
-0.04
0 0.1 0.2 0.3 0.4 0.5 0.6
Z(m)
(b)
Dispersion section with steering patterns on exit and entrance sections
0.03
0.02
0.01
0
-0.01
-0.02
-0.03
0 0.1 0.2 0.3 0.4 0.5 0.6
Z(m)
(c)

Fig. 6

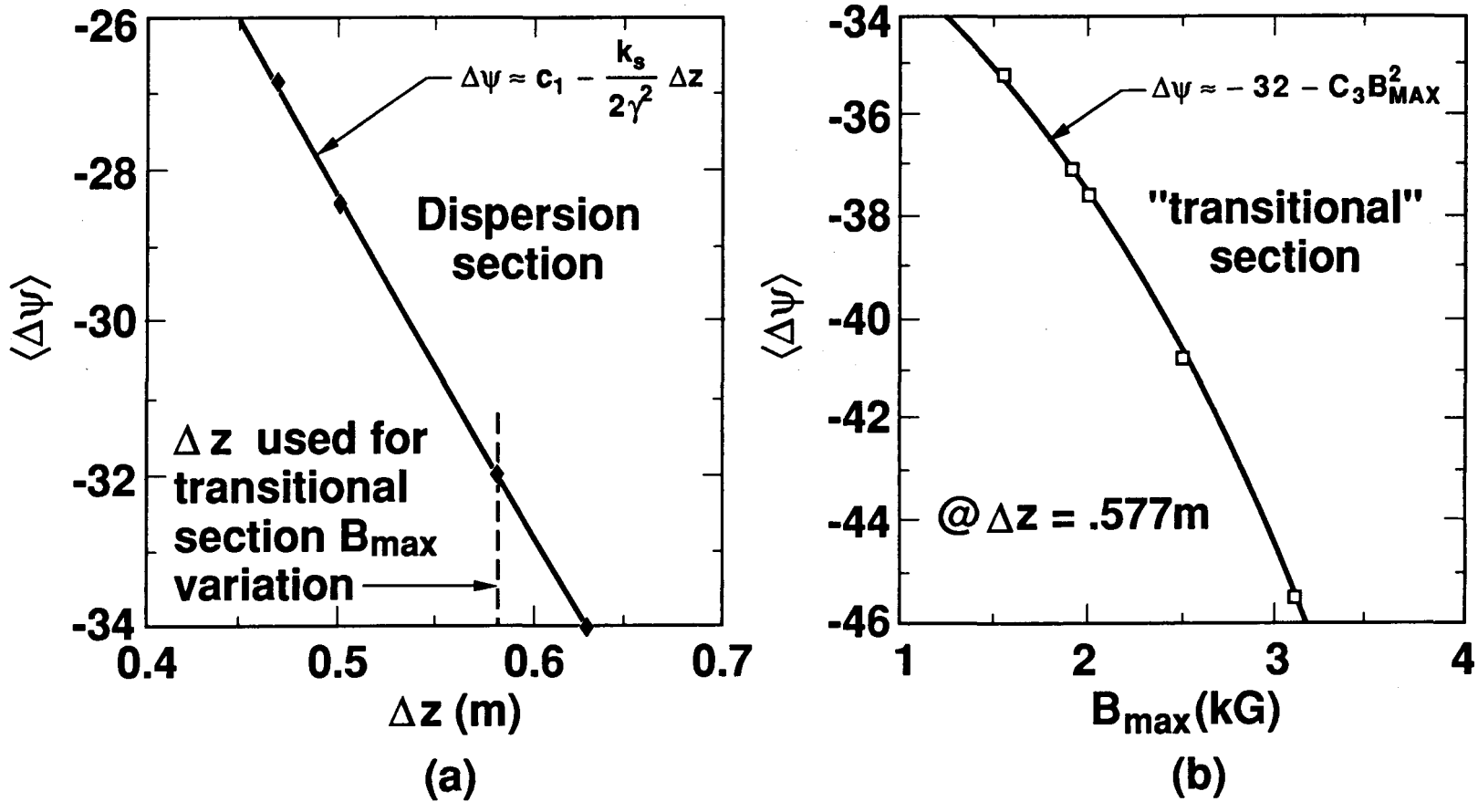
-26
-28
-30
-32
-34
⟨Δψ⟩
Δψ ≈ c1 − ks/2γ² Δz
Dispersion section
Δz used for transitional section Bmax variation
0.4
0.5
0.6
0.7
Δz (m)
(a)
-34
-36
-38
-40
-42
-44
-46
⟨Δψ⟩
Δψ ≈ − 32 − C3B²MAX
"transitional" section
@Δz = .577m
1
2
3
4
Bmax(kG)
(b)

Fig. 7

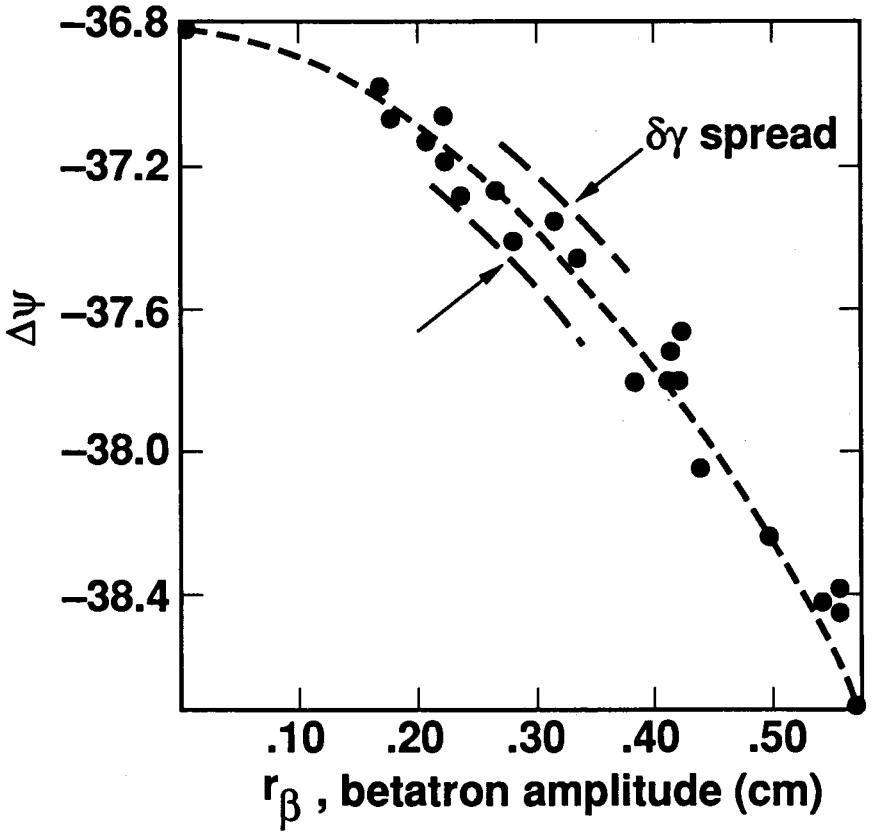
−36.8
−37.2
−37.6
−38.0
−38.4
Δψ
δγ spread
.10
.20
.30
.40
.50
r_β , betatron amplitude (cm)

Fig. 8